Electrochemical Switches Based on Ultrathin Organic Films: From Diode-like Behavior to Charge Transfer Transparency

ARTICLE *in* THE JOURNAL OF PHYSICAL CHEMISTRY C · NOVEMBER 2008

Impact Factor: 4.77 · DOI: 10.1021/jp806827a

6 AUTHORS, INCLUDING:

Noel Vincent
Paris Diderot University
56 PUBLICATIONS **842** CITATIONS
SEE PROFILE

Jalal Ghilane
Paris Diderot University
54 PUBLICATIONS **774** CITATIONS
SEE PROFILE

Hyacinthe Randriamahazaka
Paris Diderot University
80 PUBLICATIONS **1,218** CITATIONS
SEE PROFILE

Jean Christophe Lacroix
Paris Diderot University
133 PUBLICATIONS **2,725** CITATIONS
SEE PROFILE

Electrochemical Switches Based on Ultrathin Organic Films: From Diode-like Behavior to Charge Transfer Transparency

Claire Fave, Vincent Noel, Jalal Ghilane, Gaelle Trippé-Allard, Hyacinthe Randriamahazaka, and Jean Christophe Lacroix*

Interfaces, Traitements, Organisation et Dynamique des Systèmes, Université Paris 7-Denis Diderot, UMR 7086, Bâtiment Lavoisier, 15 rue Jean de Baïf, 75205 Paris Cedex 13, France

Received: July 31, 2008; Revised Manuscript Received: September 30, 2008

Ultrathin layers of thiophene derivatives were covalently attached to GC electrodes by electroreduction of diazonium salts. The films are densely packed structures and are able to mediate electron transfer above a threshold voltage tuned by the nature of the grafted molecules onto the electrode. We investigate the electron transfer properties of these layers by using electroactive probes having various redox potentials. Voltammetry and SECM measurements clearly show that for redox probes with low redox potentials diode-like behavior is observed and the current can flow in only one direction across these organic layers whereas, when the potential of the external redox probe increases, the transparency of the layers toward electron transfer in both direction increases (within the time range investigated). This behavior is not compatible with an EC_{cat} mechanism, with electroactive immobilized centers characterized by a single redox potential $E°_{Im}$, and clearly demonstrates the switching of the layer conductivity. In this sense, these layers are better modeled as covalently grafted conducting oligomers densely packed on the surface and capable of changing their charge transfer characteristics upon charge injection (i.e., doping of the grafted conjugated oligomers). The charge transfer mechanism of these ultrathin films is thus very different from that most of SAMs bearing an electroactive group, in which electron tunnelling through the monolayer is the main charge transfer mechanism.

1. Introduction

Intense research efforts are being devoted developing simple and reliable procedures to control charge transfer across interfaces. Because the molecular rectifier is a simple but vital component for molecule-based electronics, various molecules with suitable electronic asymmetry have been exploited.[1,2] Examples include electrochemical rectification on a chemically modified electrode using redox-active polymer and redox-active monolayers. Previous works by the groups of Murray[3,4] and Wrighton[5,6] have shown the great potentiality of organic thin films for controlling charge transfer at interfaces. Nevertheless, several factors may combine to limit the performance of polymer-based devices as electrochemical current rectifiers, including possible direct access of soluble redox molecules to the electrode and limitations on the magnitude of current flow that can be supported by electron hopping in the polymer layer. Accordingly, thinner rectifying layers that have more efficient blocking properties and electron transfer kinetics can potentially lead to more desirable performance characteristics. Several publications have underlined the high current rectifying properties of electroactive immobilized redox molecules grafted on dendrimers[7] or on self-assembled monolayer.[8]

Recently, we have reported the covalent modification of carbon or gold surfaces by thiophene derivatives by electroreduction of diazonium salts.[9] This method allows the preparation of very thin organic layers around 5 nm thick with covalent bonding to the electrode. The interesting point for this layer is related to its unusual electrochemical response toward ferrocene. Indeed, no current was observed on the modified electrode in the potential range where ferrocene (Fc) redox reactions usually occur on bare electrodes (which indicates that the organic layer totally blocks the electrode in this potential window) but at higher potential the current increases dramatically and an "irreversible" wave is observed with no peak for Fc^+ reduction even at very cathodic polarization during the reverse potential scan. Diode-like behavior toward ferrocene, with current flowing in only one direction, similar to that obtained by the Murray and Wrighton groups,[3−6] was thus obtained. In contrast to the usual interpretation of such effects, based on an EC_{cat} mechanism, we have proposed that this peculiar electrochemical response can be explained by assuming that these organic electrodes based on conjugated oligomers switch reversibly between conducting and totally blocking states.

In this paper, we further investigate these layers with other redox probes and show that the diode-like behavior, observed with ferrocene, is general when the probe has a low redox potential. On the other hand, when the redox potential increases, diode-like behavior disappears and the electrochemical responses of the probes are close to those observed on bare carbon. As a consequence, the organic layer appears completely "transparent" for these probes (within the time range investigated). These observations are not compatible with an EC_{cat} (or EC') mechanism and clearly demonstrate the switching of the layer conductivity. Furthermore a SECM (Scanning Electrochemical Microscopy) study, confirms switching behavior of the layers. From a practical point of view, the SECM results demonstrate that the layers are homogeneous and confirm the absence of pinholes. Then, it could be proposed as a good candidate to replace SAMs attached to gold electrodes, which often show pinhole defects in similar SECM experiments and lack stability.

* To whom correspondence should be addressed. E-mail: lacroix@univ-paris-diderot.fr.

10.1021/jp806827a CCC: $40.75
Published on Web 10/31/2008

2. Experimental Section

The 1-(2-bisthienyl)-4-aminobenzene and 1-(2-thienyl)-4-aminobenzene were synthesized following published procedure.[9,10] Ferrocene (Aldrich), thianthrene (Aldrich), decamethylferrocene (Fluka), 1,4-amino-diphenylamine (Fluka), tetrabutylamonium tetrafluoroborate (Aldrich) and lithium perchlorate (Acros) were used as received. All experiments were performed in acetonitrile (Aldrich, HPLC grade without further purification).

For electrochemical experiments, a conventional one-compartment, three-electrode cell was employed. A CHI 760C potentiostat (CH Instruments, Austin, TX) was used. The auxiliary electrode was a platinum grid; an SCE (3 M KCl) in a $CH_3OH/LiClO_4$ bridge was used as reference electrode. Working electrodes were glassy carbon (GC) discs (area = 0.07 cm^2) purchased from CH Instruments. Before use, electrodes were polished with 3 μm then 1 μm diamond paste (Struers, Denmark), ultrasonicated in analytical grade acetone for 3 min and rinsed with acetonitrile.

SECM experiments were performed in acetonitrile solution. Bu_4NBF_4 was used at 10^{-1} M as supporting electrolyte. Redox mediators were used at 10^{-3} M in SECM experiments. The platinum ultramicroelectrodes (UME) were prepared in the laboratory following a published procedure. A disk-shaped UME, 10 μm in diameter, was made by sealing platinum wires (Goodfellow) in a soft glass tube that was subsequently ground at one end. The glass edge was conically shaped with an outer diameter between 100−50 μm ($5 < RG < 10$). Prior to use, the UME was polished using diamond pastes with decreasing grain sizes. Approach curves were performed using a commercial SECM instrument with close-loop piezoelectric motors, CHI 910B (CH Instruments, Austin, TX). A three-electrode setup was employed with Ag/AgCl serving as reference electrode; a platinum wire was used as counter-electrode and a modified carbon electrode (3 mm diameter) as substrate.

3. Results

3.1. Voltammetry Measurements. Two arylthiophene diazonium salts were chosen, 1-(2-bisthienyl)-4-aminobenzene (BTAB) and 1-(2-thienyl)-4-aminobenzene (TAB). Grafted molecules will be labeled BTB and TB. In a typical experiment, modified GC electrodes were prepared by electroreduction of the diazonium salts using a previously published procedures.[9]

Fresh BTB- and TB-modified GC electrodes were immersed into decamethylferrocene (DmFc) solutions to probe their electrochemical behavior toward this reversible outer-sphere redox species. DmFc has a redox potential ($E^{0\prime} = -0.21$ V) before any charge injection into the organic layer. In both cases, the organic layer can therefore be considered to be in the "off" state for potentials where DmFc waves are seen on bare electrodes. Figure 1 compares the DmFc electrochemical response on bare, BTB-and TB-modified GC electrodes. As reference, insert Figure 1 shows the response, already published,[9] toward Fc in solution for these three electrodes.

No current is observed on either modified electrode in the classical potential range for DmFc on bare electrodes (oxidation peak at −0.14 V). On BTB- and TB-modified electrodes, the current quickly increases at higher potentials, and an irreversible oxidation wave is recorded. The oxidative peaks can be tuned according to the nature of the organic layer, as depicted in Figure 1. With BTB, the anodic peak potential is centered at 0.53 V, whereas it is at 0.73 V with a TB layer. Similar behavior has been previously reported with ferrocene[9] (0.65 V for BTB and 0.81 V for TB as compared to 0.42 V on the bare electrode). The anodic peak shape is diffusional on modified and bare GC.

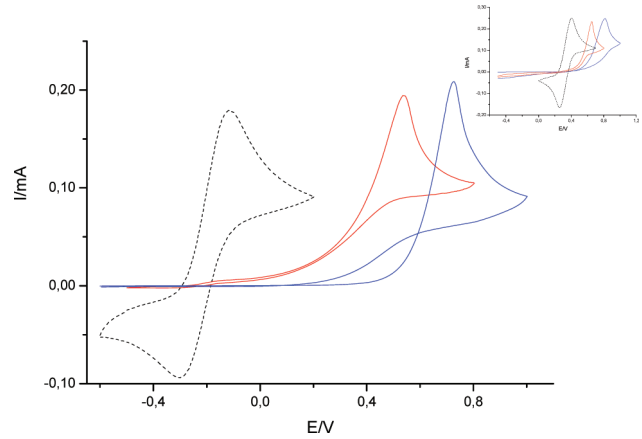

Figure 1. Cyclic voltammetry in ACN + 5. 10^{-3} M DmFc + 0.1 M $LiClO_4$ solution of bare GC (dash point), BTB-modified (red), and TB-modified (blue) electrodes. Scan rate v = 0.1 V/s. Inset: Cyclic voltammetry in ACN + 0.01 M Fc + 0.1 M $LiClO_4$ solution of bare GC (dash point), BTB-modified (red), and TB-modified (blue) TB electrodes.[9]

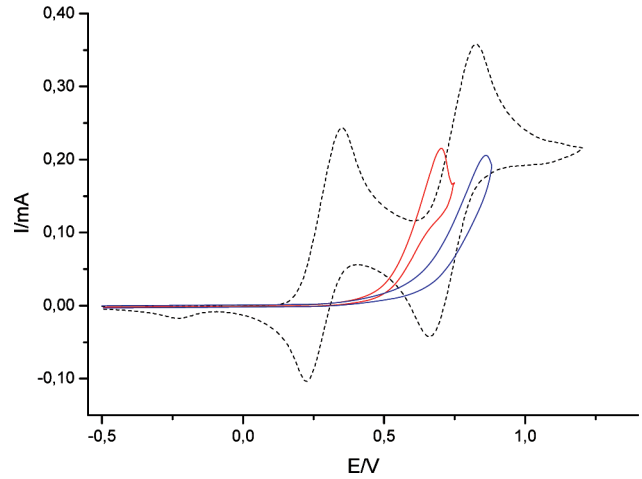

Figure 2. Cyclic voltammetry in ACN + 0.01 M ADPA + 0.1 M $LiClO_4$ solution showing the responses of $ADPA^+$/ADPA and $ADPA^{2+}$/$ADPA^+$ on bare GC (dash point), $ADPA^+$/ADPA on BTB-modified (red), and $ADPA^+$/ADPA TB-modified (blue) electrodes. Scan rate v = 0.1 V/s.

For both electrodes, the response is stable upon successive scans. These experiments are in complete agreement with those obtained previously when using Fc as redox probe. The CV obtained in the case of TB-modified electrode using decamethylferrocene as redox couple show frequently a cross-over. This behavior is not yet fully understood but may be attributed to an enhancement of the electroactive surface which induces the increase of the current during the backward scan as already seen in the case of conducting polymers.[11]

The next step was the use of redox species with two successive oxidative waves, the first one being at a potential close to that of Fc, the second one in a region where charges have been injected into the organic layer, as judged by the CV response of the film in 0.1 M $LiClO_4$ acetonitrile solution.[9] We used 1,4-amino-diphenylamine (ADPA) which presents two anodic peak potentials at 0.35 and 0.83 V on bare GC. In Figure 2, the response of the two organic modified electrodes was probed from −0.5 to 0.7 V for BTB or 0.8 V for TB in order to record the behavior corresponding to the first redox system: $ADPA^+$/ADPA. This potential range is similar to that used with Fc or DmFc. In both cases, we obtain an irreversible wave with

SCHEME 1

$$BTB \rightarrow BTB^{+\cdot} + e^{-} \quad (1)$$

$$BTB^{+\cdot} + Fc \rightarrow BTB + Fc^{+} \quad (2)$$

an oxidative shift of the peak (0.71 V for BTB and 0.83 V for TB) and with a very similar shape.

All these results are in agreement with those obtained previously with Fc and confirm the particular behavior of these organic layers. As illustrated above, for the three redox probes (Fc^+/Fc, $DmFc^+$/DmFc, and $ADPA^+$/ADPA couples), a similar electrochemical diode behavior is thus observed and the current flows in only one direction. The BTB and TB layers of nanometric thickness act as current rectifiers.

As already stated, many devices, with this behavior, have been prepared from electrodes modified with redox polymer films. The main mechanism used to describe charge transfer between a redox polymer or an electroactive monolayer and a diffusive redox probe is the Electrochemical Chemical EC_{cat} mechanism[12−14] including an outer-sphere electron transfer reaction between the metal and the immobilized redox group and a bimolecular chemical reaction between the immobilized and the free diffusive probe (Scheme 1.)

The EC_{cat} mechanism allows to fit most of electrochemical data obtained with monolayers bearing a terminal electroactive function in the presence of free redox probe.[7,15] In this case, the recorded catalytic current is due to the enhanced electroactivity of the monolayer. In our case, the current is limited by the mass transport (diffusion) showing $I_p = f(v^{1/2})$ (for the low scan rates investigated) and varies linearly with the bulk concentration of the probe (data not shown). In fact, for the EC_{cat} mechanism, the chemical step is thermodynamically promoted only for probes having an $E^{0\prime}$ less than that of the redox centers immobilized in the film (E^0_{Im}). For $E^{0\prime} > E^0_{Im}$ the EC_{cat} model predicts a rate constant close to zero and, consequently, the absence of charge transfer and of electrochemical signals. In other words, when the redox probe has a potential above that of the immobilized redox species and within the framework of this mechanism, it is not possible to oxidize the redox probe in the solution, the diode-like behavior disappears and current flow is impossible in both directions. We then investigated the electrochemical response of redox probes with higher redox potentials.

The ADPA redox probe presents a second oxidation peak ($ADPA^{2+}$/$ADPA^+$ couple) at 0.83 V on GC. Cyclic voltammograms, recorded from −0.5 to 1.0 V for BTB or 1.2 V for TB, present small anodic shifts of the oxidative peak potentials of this redox couple at 0.91 and 0.95 V, respectively, compared to those obtained on GC (cf. Figure 3). However, the most important difference is that, contrary to the results previously obtained, the electrochemical signal starts to be reversible with reduction peaks occurring at potentials close to that observed on a bare electrode. These quasi-reversible voltammetric waves of the second electron transfer of ADPA (Figure 3) obtained on BTB- and TB-modified electrode, reduce the possibility to have a classical EC_{cat} mechanism.

Thianthrene (Th) is another reversible system with a redox potential at 1.13 V on GC, above that of $ADPA^{2+}$/$ADPA^+$. Figure 4 shows the recorded response. It can be seen that on BTB the response is reversible and is very similar to that obtained on bare GC. On the contrary, the response obtained on TB film remains irreversible.

In the case of thianthrene as redox couple on TB layer, the peak is not shifted compare to that obtained on bare GC.

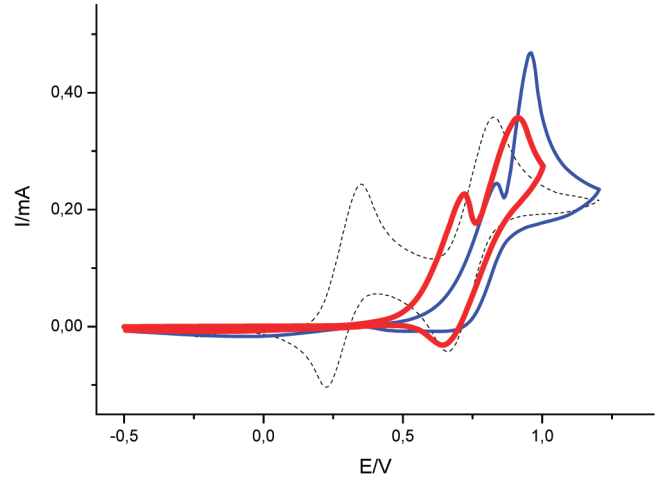

Figure 3. Cyclic voltammetry in ACN + 0.01 M ADPA + 0.1 M $LiClO_4$ solution of bare GC (dash point), BTB-modified (red), and TB-modified (blue) electrodes. Scan rate $v = 0.1$ V/s.

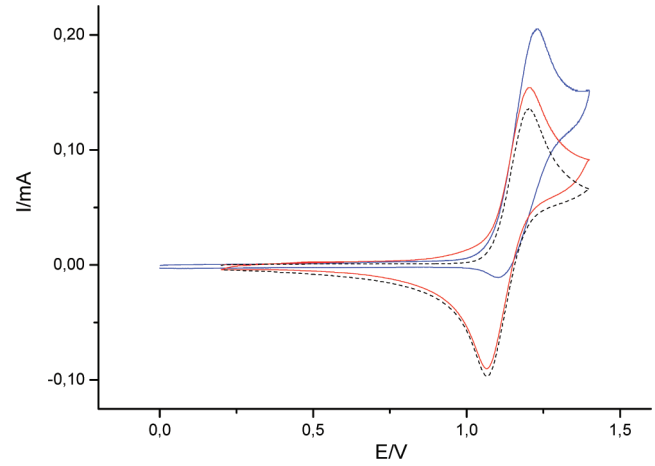

Figure 4. Cyclic voltammetry in ACN + 5.10^{-3} M Th + 0.1 M $LiClO_4$ solution of bare GC (dash point), BTB-modified (red), and TB-modified (blue) electrodes. Scan rate $v = 0.1$ V/s.

Therefore, the magnitude of the anodic shift decreases when the standard potential of the redox probe is more positive. This behavior reflects the fact that the conductivity of the organic thin-film increases when the potential is more positive (anodic) than the threshold potential E_{th}. However, an anodic shift is observed for decamethyl ferrocene, ferrocene, and the first oxidation of ADPA redox couples. These behaviors indicate a partial control of the organic film in the charge transfer. On the other hand, when the value of $E^{0\prime}$ is high enough to have a large amount of charges injected into the film, the organic thin-film no longer controls the heterogeneous electron transfer. In this case, the anodic shift disappears. This trend is observed for thianthrene on TB and BTB.

It can thus be concluded that when the redox probe potential increases and is now in the range where a large amount of charge has been injected into the organic layer, the diode-like behavior disappears and current flows in both directions. As a consequence, the organic layer appears to be completely "transparent" for these redox probes (within the time range investigated). These observations are not compatible with an EC_{cat} mechanism with electroactive immobilized centers characterized by a single E°_{Im}, and clearly demonstrate the switching of the layer conductivity.

3.2. SECM Investigations. The major advantage of this technique is to provide a localized examination of the redox

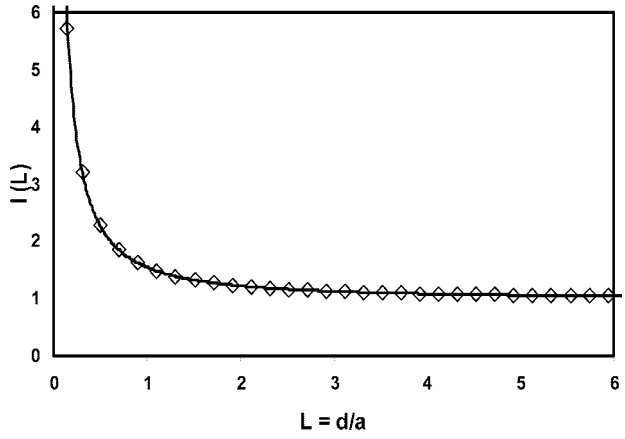

Figure 5. (◇) Experimental approach curve of Pt UME above carbon substrate in ACN solution containing 10^{-3} M Fc and 10^{-1} M Bu_4NBF_4. (−) Theoretical approach curve for a conducting substrate.

properties of the surface down to the submicrometer scale and to probe the modified surface from the solution side. From that point and the results obtained by cyclic voltammetry, it comes into view to be useful to investigate the grafted BTB layer onto GC using SECM.[16]

In preliminary experiments, approach curves were achieved with Fc and Th as mediators using carbon electrode as substrate; the potential applied to the UME is 0.5 and 1.3 V for Fc and Th, respectively. Under our experimental conditions the GC substrate is not electrically connected. Figure 5 shows the experimental approach curve obtained with Fc as mediator using a GC electrode. For normalized distance $L > 3$, $I(L)$ is close to unity. This value reflects the absence of interaction between the Fc^+ electrogenerated at the UME and the substrate for this distance. As expected, for $L < 3$, the current increases rapidly and positive feedback is observed. This enhancement demonstrates the regeneration of the mediator at the GC electrode. Furthermore, the SECM investigation was performed using Th as mediator and the same approach curve was obtained (data not shown). All experimental approach curves are in good agreement with the theoretical curve expected for a conducting substrate under diffusion control.

Figure 6 illustrates the experimental approach curves recorded above the BTB-modified electrode using two redox couples, Fc^+/Fc (figure 6A) and Th^+/Th (Figure 6B). The approach curve shows that the normalized current falls rapidly for the first mediator (Figure 6A) when L decreases, and is in good agreement with the theoretical variation expected for an insulating substrate (negative feedback), demonstrating the insulating properties of the TB and BTB layers under these conditions.

To check the homogeneity of the BTB layer, approach curve was recorded in different areas of the surface and the same behavior was observed. These results demonstrate that the BTB layer is homogeneous above the GC substrate and has no pinholes at the micrometer size. It is well-known that with 10 μm tip it should be possible to identify pinholes 20 times smaller than the size of the tip, in our case corresponding to 500 nm. [16] In addition, the approach curve was also achieved above the BTB layer using a smaller tip, 1 μm diameter, and the same data as shown in Figure 6A are obtained. Thus, the obtained negative feedback, in such experimental conditions, indicates the absence of pinholes in the BTB layer with diameter higher than 50 nm.

Figure 6B illustrates the experimental approach curve recorded above the BTB-modified electrode using the Th^+/Th couple as mediator. The approach curve shows that the normalized current increases rapidly when L decreases for this second mediator, in sharp contrast with the behavior when Fc^+/Fc is used. Furthermore, the approach curve is in a good agreement with the theoretical variation expected for a conducting substrate (positive feedback), demonstrating that the BTB layer displays conducting properties under these conditions. Switching from Th^+/Th to Fc^+/Fc and then to Th^+/Th as mediators in successive experiments on the same BTB layer makes it possible to record approach curves switching from positive to negative and back to positive feedback. Approach curves for different areas of the surface with Fc^+/Fc mediator again demonstrate that the BTB layer is homogeneous above the GC substrate and that no pinholes are seen or created when the layer is submitted to Th^+/Th mediator.

The SECM results fully agree with the results obtained using cyclic voltammetry and indicate clearly that, depending on the redox probe potentials, the current flows only in one direction or in both directions. In the first case, the organic layer appears to be completely insulating for the reduction of the mediator, avoid the penetration of the probe toward the underlying GC substrate and do not yield to its regeneration. In the second case, the BTB film relays the electron transfer between the film/solution interface and the electrode/film interface (within the time range investigated), regenerating the mediator.

3.3. Qualitative Variation of the Apparent Charge Transfer Rate on Modified Electrode. To investigate further the charge transfer of the TB and BTB layers with a mobile redox probe, the variation of the anodic peak potential of the different redox probes was followed. For the non reversible redox reactions, kinetic parameters such as the apparent electronic rate constant (k^0_{app}) and the electron-transfer coefficient (α) can be determined by measuring the variation of peak potential splitting (ΔE_p) with the scan rate according to classical methods.[17] In

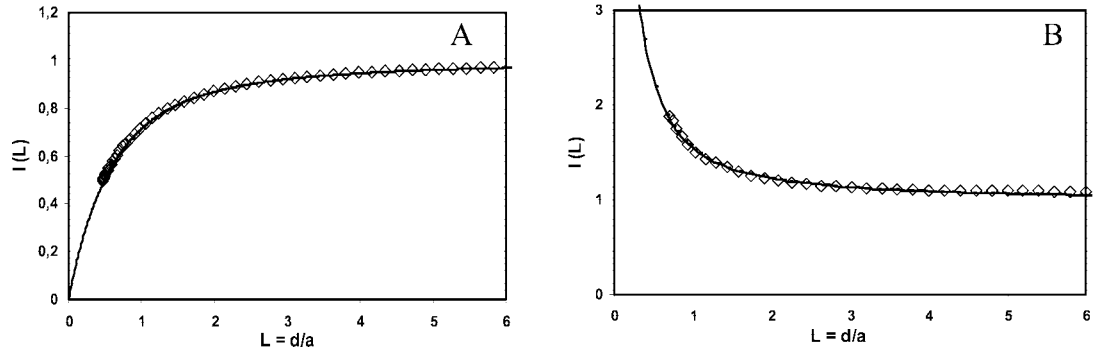

Figure 6. (◇) Experimental approach curves of Pt UME above BTB-modified GC substrate in ACN solution containing 10^{-1} M Bu_4NBF_4. (A) 10^{-3} M Fc^+/Fc and (B) 10^{-3} M Th^+/Th. (−) Theoretical approach curve for an insulating or conducting substrate.

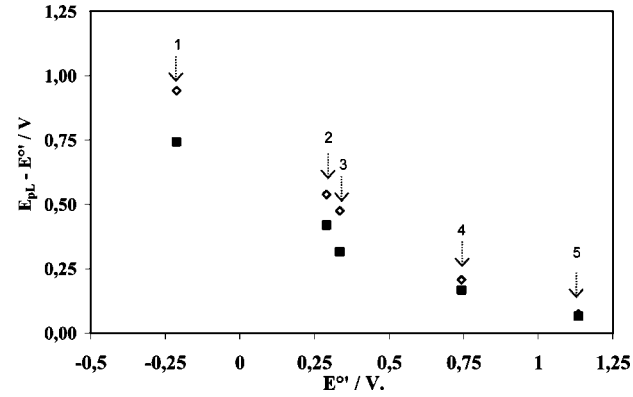

Figure 7. Difference between the probe anodic peak, E_{pL} and $E^{0\prime}$, on (◇) TB or (■) BTB as a function of $E^{0\prime}$ with $\upsilon = 100$ mV/s. (1) $DmFc^+$/DmFc, (2) $ADPA^+$/ADPA, (3) Fc^+/Fc, (4) $ADPA^{2+}/ADPA^+$, (5) Th^+/Th.

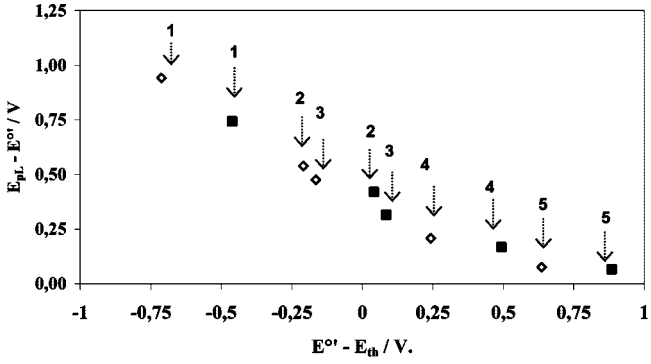

Figure 8. Difference between the probe anodic peak E_{pL} and $E^{0\prime}$ on (◇) TB or (■) BTB as a function of $(E^{0\prime} - E_{th})$ with $\upsilon = 100$ mV/s. (1) $DmFc^+$/DmFc, (2) $ADPA^+$/ADPA, (3) Fc^+/Fc, (4) $ADPA^{2+}/ADPA^+$, (5) Th^+/Th.

our case, the absence of the back-reaction does not allow such a determination (or it can be done by assuming that the lack of backward peak in due to the blocking effect of the insulating organic layer).

Thus, in a first intention, we decided to study the variation $(E_{pL} - E^{0\prime})$ of the difference between the anodic peak potential E_{pL} of the probe on modified electrodes (L = TB or BTB) and $E^{0\prime}$ with respect to their respective $E^{0\prime}$ deduced from measurements with each probe on bare GC. For a constant scan rate and a given redox probe, an increase in $(E_{pL} - E^{0\prime})$ indicates a decrease of k^0_{app}.[16] In fact, $(E_{pL} - E^{0\prime})$ increases as the dimensionless parameter Λ decreases, $(\Lambda = k^0_{app}\sqrt{RT/nF\upsilon D})$ where k^0_{app} is the apparent rate constant at zero overpotential, D the probe diffusion coefficient, and υ the scan rate. Hence, the difference $(E_{pL} - E^{0\prime})$ gives qualitative information about k^0_{app} of probes on TB and BTB layers and the variation of $(E_{pL} - E^{0\prime})$ could be correlated with the change in k^0_{app}. Figure 7 shows the variation of $(E_{pL} - E^{0\prime})$ as a function of $E^{0\prime}$ for the different probes used such as Fc, DmFc, ADPA (first and second redox system), and Th.

One observes that $(E_{pL} - E^{0\prime})$ decreases for both TB- and BTB-modified electrodes as $E^{0\prime}$ of the probe shifts to more anodic values. This trend indicates that k^0_{app} increases when $E^{0\prime}$ shifts toward the anodic potentials.

To take into account the respective threshold potentials of BTB and TB ($E_{th} = 0.25$ and 0.5 V, respectively), defined as the potential above which charges start to be injected into the organic layer (These value have already been determined in a previous work[9] from the CV curves of BTB- and TB-modified electrodes in an ACN + $LiClO_4$ solution), we plot $(E_{pL} - E^{0\prime})$ as a function of $(E^{0\prime} - E_{th})$ (Figure 8). This representation allows to study the $(E_{pL} - E^{0\prime})$ difference with respect to the threshold potential of each layer, E_{th}, and to perform a discussion whatever their values.

Figure 8 shows that taking $(E^{0\prime} - E_{th})$ as abscissa allows us to visualize into all the experimental points on the same curve. This result indicates that the same process or mechanism occurs on both TB and BTB layers. The chemical structure of the layers does not basically influence their behavior; only E_{th} is modulated.

In a second intention, and despite the fact that the absence of the back-reaction does not allow the determination of kinetic parameters, by measuring the variation of the peak potential splitting (ΔE_p) with the scan rate according to classical methods,[18,19] we can determine the apparent charge transfer rate constant k^0_{app} from the values of the peak potentials. To this end, we assume that k^0_{app} can be determined from a modified simple E mechanism in which the modified electrode is totally blocked below the threshold potential E_{th}. Also, mass transfer is controlled by the diffusion, and no notable adsorption of the mobile electroactive species occurs. We know that this model is oversimplified but it is helpful for rationalizing the obtained data. From CV data, we determine the charge transfer rate constant k^0 for the bare CG electrode, and the apparent charge transfer rate constante k^0_{app} for the modified electrode. Then, we report the ratio k^0_{app}/k^0 allowing to analyze the relative change in the charge transfer rate constant. In Figure 9, we observe that k^0_{app}/k^0 depends strongly upon the value of $E^{0\prime}$, relative to E_{th}.

For $E^{0\prime} < E_{th}$, the rate constant is drastically reduced compared to bare GC. On the other hand, no notable change in k^0_{app} is observed for $E^{0\prime} \gg E_{th}$ (Figure 10). In this latter case, the ultrathin organic layer seems to be transparent and does not hinder charge transfer. In other words, the ultrathin organic layer can be viewed as a supplementary energetic barrier to heterogeneous electron transfer when $E_{th} > E^{0\prime}$.

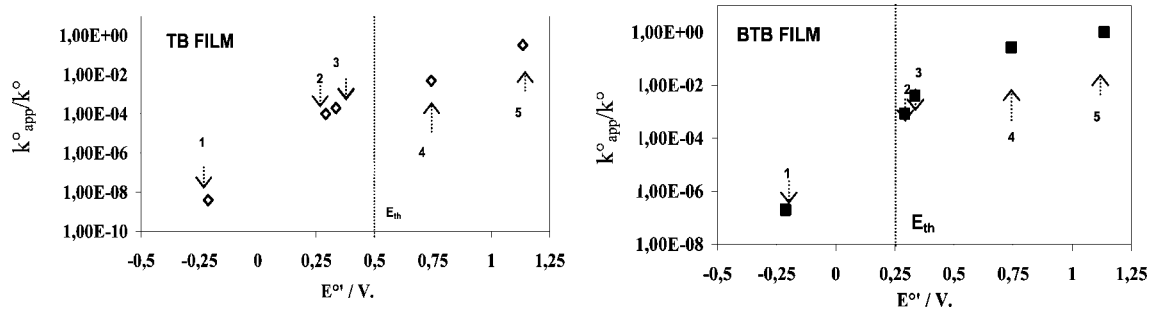

Figure 9. Variation of k^0_{app}/k^0 as a function of the redox potential $E^{0\prime}$ of the electroactive probe on TB (left), and BTB films (right). (1) $DmFc^+$/DmFc, (2) $ADPA^+$/ADPA, (3) Fc^+/Fc, (4) $ADPA^{2+}/ADPA^+$, (5) Th^+/Th.

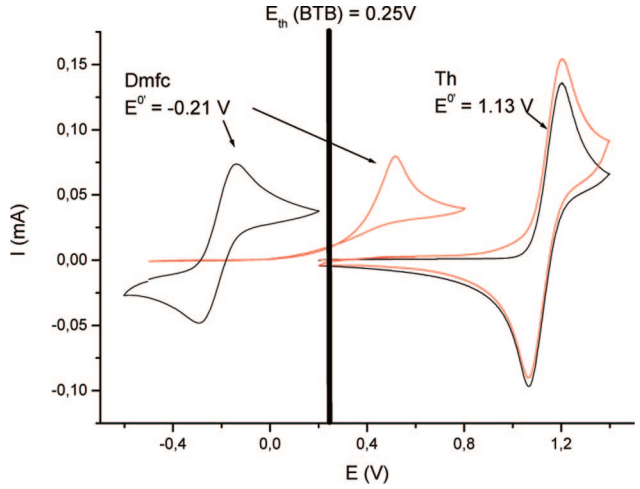

Figure 10. Cyclic voltammetry in ACN + 0.1 M $LiClO_4$ solution of bare GC (black) and BTB-modified (red) electrodes for $DmFc^+$/DmFc and Th^+/Th. $\upsilon = 0.1$ V/s.

An alternative to the EC_{cat} mechanism could be the model of heterogeneous charge transfer reaction at highly doped organic semiconductor interfaces. In such a case, the charge transfer kinetics is described as a bimolecular redox reaction depending on the concentrations of charge carrier and free redox probe at the film/solution interface. It is assumed that the interfacial probe concentration does not depend on the probe, the evolution of E_{pL} with $E^{0\prime}$ could be due to a difference of interfacial charge carieers. A model taking into account the interfacial density of charge carriers and the apparent electronic transfer evolutions as a function of the applied potential is under construction and will be the subject of a forthcoming paper. It is also likely that the dynamics of charge injection into the grafted organic layers may affect the electrochemical responses reported here, which were observed at low scan rates. Investigation of high scan rate response will also be reported elsewhere.

4. Conclusion

We have investigated the electrochemical behaviors of ultrathin layers of thiophene derivatives that have been covalently attached to GC electrodes through the electroreduction of diazonium salts. The thickness of TB and BTB layers is around 4 and 5 nm. This high value prevents direct tunnelling between the GC electrode and the free redox probe located near the layer/solution interface. Moreover, the densely packed structure (no pinholes, as evidenced using SECM) hinders the possibility for the free redox probes to diffuse through the layer in order to minimize the electron tunnelling distance. Then, the charge transfer mechanism of TB and BTB is very different from that of most SAMs bearing an electroactive group, in which electron tunnelling through the monolayer is the main charge transfer mechanism. Indeed, for redox probes with low redox potentials diode-like behavior is observed, and the current can flow in only one direction across these organic layers whereas, when the potential of the external redox probe increases, the transparency of the layers toward electron transfer in both directions increases (at low scan rates). This behavior is not compatible with an EC_{cat} mechanism with electroactive immobilized centers characterized by a single $E°_{Im}$, and clearly demonstrates the switching of the layer conductivity. In this sense, these layers are better modeled as covalently grafted conducting oligomers densely packed on the surface and capable of changing their charge transfer characteristics upon charge injection (i.e., doping of the grafted conjugated oligomers)

Acknowledgment. This work was supported by the ANR Program (06 0296) administered through the French Research Ministry. We are particularly grateful to Dr. J. S. Lomas for revising our text and correcting the English.

References and Notes

(1) Aviram, A.; Ratner, M. A. *Chem. Phys. Lett.* **1974**, *29*, 277.
(2) Metzger, R. M. *Chem. Rev.* **2003**, *103*, 3803.
(3) Murray, R. W. *Philos. Trans. R. Soc. London, Ser. A: Math., Phys. Eng. Sci.* **1981**, *302*, 253.
(4) Chidsey, C. E. D.; Murray, R. W. *Science* **1986**, *231*, 25.
(5) Wrighton, M. S. *Science* **1986**, *231*, 32.
(6) Smith, D. K.; Lane, G. A.; Wrighton, M. S. *J. Am. Chem. Soc.* **1986**, *108*, 3522.
(7) Oh, S. K.; Baker, L. A.; Crooks, R. M. *Langmuir* **2002**, *18*, 6981.
(8) Alleman, K. S.; Weber, K.; Creager, S. E. *J. Phys. Chem.* **1996**, *100*, 17050.
(9) Fave, C.; Leroux, Y.; Trippé, G.; Randriamahazaka, H.; Noel, V.; Lacroix, J. C. *J. Am. Chem. Soc.* **2007**, *129*, 1890.
(10) Tan, L.-S.; Nagvekar, D. S.; Sankaran, B. *US Patent* **2000**, *6*, 130–339.
(11) Downard, A. T.; Pletcher, D. *J. Electroanal. Chem.* **1986**, *206*, 147.
(12) Lyons, M. E. G. *Sensors* **2001**, *1*, 215.
(13) Creager, S. E.; Radford, P. T. *J. Electroanal. Chem.* **2001**, *500*, 21.
(14) Andrieux, C. P.; Dumas-Bouchiat, J. M.; Savéant, J. M. *J. Electroanal. Chem.* **1982**, *131*, 1.
(15) (a) Xie, Y.; Anson, F. C. *J. Electroanal. Chem.* **1995**, *384*, 145. (b) Amarasinghe, S.; Chen, T.; Moberg, P.; Paul, H. J.; Tinoco, F.; Zook, L. A.; Leddy, J. *Anal. Chim. Acta* **1995**, *307*, 227. (c) Berchmans, S.; Ramalechume, C.; Lakshmi, V.; Yegnaraman, V. *J. Mater. Chem.* **2002**, *12*, 2538.
(16) Bard, A. J.; Mirkin, M. V. *Scanning Electrochemical Microscopy*; Marcel Dekker: New York, 2001.
(17) Nicholson, R. S. *Anal. Chem.* **1966**, *38*, 370.
(18) Bard, A. J.; Faulkner, L. R. *Electrochemical Methods: Fundamentals and Applications*, 2nd ed.; John Wiley and Sons: New York, 2001; p 236.
(19) Nicholson, R. S. *Anal. Chem.* **1965**, *37*, 1351.

JP806827A